Transactions of the VSB - Technical University of Ostrava Vol. XV, No. 1, 2020
Safety Engineering Series, ISSN 1805-3238 pp. 38-46, DOI 10.35182/tses-2020-0005

COMPARISON OF VARIOUS APPROACHES FOR DETERMINATION OF SEPARATION DISTANCES

Daniela PITELKOVÁ[1], Petr HEJTMÁNEK[2], Vladimír MÓZER[3]

Research article

Abstract: The extent of fire spread by radiation is delimited by separation distances, required to prevent external fire spread due to excessive radiation heat or falling burning brands. The simplified calculation method uses a series of precalculated tabulated values. Alternatively, a more precise analytical calculation approach can be used. The resolution of the method can determine the required separation distances significantly. This paper evaluates analytical calculation methods and CFD simulations to determine their accuracy of separation distances prediction. The most appropriate are standard analytical calculation methods with sufficient number of evaluation points along the radiating surface.

Keywords: Separation distances, Fire spread zone, Stefan-Boltzmann law, View factor, Radiation intensity.

Introduction

A zone of potential fire spread is present around a building in fire. This zone is bound by separation distances, beyond which fire spread risk is considered sufficiently low. Inside the zone fire may spread by radiant heat or falling burning brands.

Separation distances are hence an important aspect of building fire safety design in the dense urban areas. The primary goal is to avoid potential fire spread among the buildings, which becomes a problem on small lots where buildings are placed close to the property boundaries.

According to the Czech technical standards (ČSN 73 0802 (ČSN 73 0802, 2020) and ČSN 73 0804 (ČSN 73 0804, 2020)), the zone of potential fire spread must not extend beyond the property boundaries of the owner. There are a few exceptions from this requirement, such as the projection of the zone onto the public areas, such as roads, pavements and other similar areas where fire spread is not expected. Nonetheless, the zone cannot project onto a private property, regardless of its use, unless the owner of the affected property agrees and building control approves such exemption. In any case, it is always advisable that the zone of potential fire spread does not extend beyond the property on which the considered building is located, and does not affect neighbouring buildings, regardless of their ownership.

Separation distances are determined by two methods in the Czech Republic. The first method is a simplified approach which uses tabulated precalculated values from the technical standards for building fire safety design ČSN 73 0802 (ČSN 73 0802, 2020), ČSN 73 0804 (ČSN 73 0804, 2020). The second method is more precise and uses analytical calculation approach based, the description of which may be found in ČSN EN 1991-1-2 (ČSN EN 1991-1-2, 2004) and (Reichel, 1989). The critical heat radiation intensity in this case is taken from ČSN 73 0802 (ČSN 73 0802, 2020), ČSN 73 0804 (ČSN 73 0804, 2020).

The simplified approach takes the point with the highest intensity of heat radiation, usually the centre of the radiating surface, and applies the required separation distance to the entire radiating surface. This means that the separation distance is overestimated, particularly at the edges of the radiating surface, however, errs on the side of safety.

[1] Faculty of Civil Enginering, Czech Technical University in Prague, Prague, Czech Republic, daniela.pitelkova@cvut.cz

[2] Faculty of Civil Enginering, Czech Technical University in Prague, Prague, Czech Republic, petr.hejtmanek@cvut.cz

[3] Faculty of Civil Enginering, Czech Technical University in Prague, Prague, Czech Republic, vladimir.mozer@cvut.cz

There is no universal internationally applied method for the determination of sufficient separation distances. Nonetheless the majority of the methods are based on the physics laws of radiative heat transfer. They also use, implicitly or explicitly, different critical radiation intensities considered as limits for fire spread.

The separation distances are usually dependent primarily on the radiation intensity, which is described through the Stefan-Boltzmann law. In practice, the law can be mathematically expressed through the equation of the intensity of radiant heat flux (Blahož and Kadlec, 1996; Kučera, 2009):

$$I = \sigma \cdot \varepsilon \cdot \phi \cdot [(T_N + 273)^4 - (T_0 + 273)^4] \quad [\text{kW.m}^{-2}] \ (1)$$

where

$\sigma = 5{,}67 \cdot 10^{-8}$ [W.m^{-2}.K^{-4}] Stefan-Boltzmann constant;

ε emissivity [-];

ϕ view factor [-];

T_N gas temperature inside fire compartment [°C];

T_0 initial temperature (usually 20 °C) [°C].

The intensity of radiant heat flux is calculated from the temperature of burning gases in the fire enclosure or compartment. This temperature - T_N - may be established in various ways. A simplified way for determination of T_N for a given time is to use the ISO 834 time-temperature curve relationship (ČSN 73 0802, 2020):

$$T_N = T_0 + 345 \cdot \log(8t + 1) \quad [\text{°C}] \ (2)$$

where

t time [minutes];

T_0 initial temperature (usually 20 °C) [°C].

Along with the temperature of the emitting surfaces (equal to the gas temperature inside the fire enclosure), the view factor has a significant impact on the resulting radiant heat flux at the receiving surface. The view factor is dependent on the following:

- shape and size of the emitting and receiving surfaces;
- distance between the emitting and receiving surfaces;
- mutual orientation (angle) of the emitting and receiving surfaces.

The view factor is calculated differently for various combinations of shapes and orientations of the emitting and receiving surfaces.

The basic configuration (as per ČSN 73 0802 (ČSN 73 0802, 2020), ČSN 73 0804 (ČSN 73 0804, 2020)) is a parallel configuration of the emitting and receiving surfaces. It is representative of a case of two building exterior walls parallel to each other. For an exposure point of view, this configuration also represents the most severe exposure along the emitting surface width.

The partial view factors for this configuration are calculated as follows:

$$\phi_i = \frac{1}{2\pi} \cdot \left[\frac{a}{\left(1 + a^2\right)^{1/2}} \cdot \tan^{-1}\left(\frac{b}{\left(1 + a^2\right)^{1/2}} \right) + \frac{b}{\left(1 + b^2\right)^{1/2}} \cdot \tan^{-1}\left(\frac{b}{\left(1 + b^2\right)^{1/2}} \right) \right] \quad [-] \ (3)$$

where

$a = h/s$;

$b = w/s$;

s (separation) distance between the radiating and receiving surfaces [m];

h height of the i-th segment (1, 2, 3, 4) of the radiating surface [m];

w width of the i-th segment of radiating surface [m].

Subsequently the resulting view factors for the entire radiating surface (opening) is calculated in three different ways, depending on the location of the element representing the receiving surface:

1. view factors for the receiving surface directly opposing the radiating surface (opening) - Fig. 1 a):

$$\phi = \phi_1 + \phi_2 + \phi_3 + \phi_4 \quad [-] \ (4)$$

2. view factors for the receiving surface directly opposing the radiating surface (opening) - Fig. 1 b):

$$\phi = \phi_1 + \phi_2 \quad [-] \ (5)$$

3. view factors for the receiving surface beyond the edges away from the radiating surface (opening) - Fig. 1 c):

$$\phi = \phi_{ABEF} + \phi_{BCDE} - \phi_3 - \phi_4 \quad [-] \ (6)$$

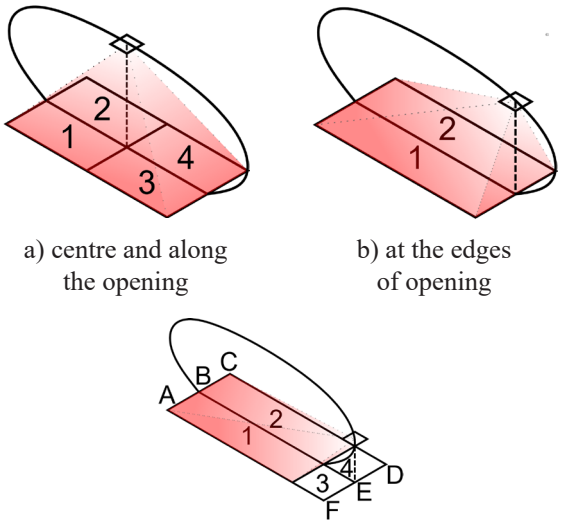

a) centre and along the opening

b) at the edges of opening

c) beyond the edges of opening

Fig. 1 Possible configurations for calculation of the view factor for the emitting surface

The view factor for two surfaces with an angle θ (Fig. 2) can be calculated as follows (ČSN EN 1991-1-2, 2004) with Equation (7).

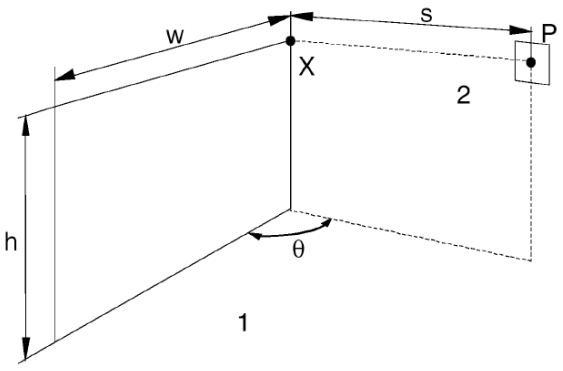

Fig. 2 Configuration for calculation of view factor of receiving and emitting surfaces with angle θ (ČSN EN 1991-1-2, 2004)

From the overall radiation intensity directly at the emitting surface and the required critical radiation intensity, the critical view factor can be established:

$$\phi_c = \frac{I}{I_c} \quad [-] \ (8)$$

where

I_c critical radiation intensity (13-18.5 (Reichel, 1989)) [kW.m^{-2}].

The separation distance s (see equation (7)), i.e. the distance at which the radiation intensity decreases to the required critical radiation intensity, is reached when:

$$\phi \le \phi_c \quad (9)$$

From the engineering perspective, there is a number of approaches of implementing the above calculation procedure. They differ in accuracy, primarily due to reduction of the number of points of the emitting surface evaluated.

Methods

The technical standards for building fire safety design in the Czech Republic are based on the principles described above. Detailed description of individual approaches may be found for example in ČSN 73 0802, ČSN 73 0804 and ČSN EN 1991-1-2.

The evaluation of the different approaches is based on a simple model case with a single opening, which represents the radiation emitting surface. The focus was put on the extent and shape of the zone in which the radiation intensity was above the critical limit 18.5 kW.m^{-2}, which was taken from ČSN 73 0802 and ČSN 73 0804 (ČSN 73 0802, 2020; ČSN 73 0804, 2020).

$$\phi = \frac{1}{2\pi} \cdot \left[\tan^{-1}(a) - \frac{(1 - b\cos\theta)}{(1 + b^2 - 2b\cos\theta)^{1/2}} \cdot \tan^{-1}\left(\frac{a}{(1 + b^2 - 2b\cos\theta)^{1/2}} \right) + \frac{a}{(a^2 + \sin^2\theta)^{1/2}} \cdot \left[\tan^{-1}\left(\frac{(b - \cos\theta)}{(a^2 + \sin^2\theta)^{1/2}} \right) + \tan^{-1}\left(\frac{\cos\theta}{(a^2 + \sin^2\theta)^{1/2}} \right) \right] \right] \quad [-] \ (7)$$

where

$a = h/s$;

$b = w/s$;

s (separation) distance between the radiating and receiving surfaces [m];

h height of the i-th segment (1, 2, 3, 4) of the radiating surface [m];

w width of the i-th segment of the radiating surface [m];

θ angle between the radiating and receiving surface.

Safety Engineering Series, ISSN 1805-3238 pp. 38-46, DOI 10.35182/tses-2020-0005

The height of the opening was constant - 1.25 m; this represents a standard window height found in many buildings. The width of the opening was gradually increased from 1.0 m to 3.0 m in increments of 0.5 m.

To calculate the radiation intensity, which increases with time - see equations (1) and (2), fire duration was taken as 45 minutes. This value is representative of dwelling houses and residential accommodation as per ČSN 73 0802. The fire duration of 45 minutes corresponds to the temperature T_N = 902.32 °C and to the radiation intensity at the emitting surface I = 108.5 kW.m^{-2}.

The individual approaches to the determination of the separation distance s evaluated were as follows:

Method 1 - tabulated data method from ČSN 73 0802 with interpolation (Fig. 3 a) - the tabulated values of separation distances are established for the radiating surface centre point (horizontally and vertically), using view factor calculation configuration shown in Fig. 1 a);

Method 2 - detailed calculation based on the points positioned along the opening horizontal centreline in the middle and at the edges with the approximation of the side extent by a semi-circular shape (Pokorný, 2017) (Fig. 3 b) - the values of separation distances are established for the radiating surface horizontal centre line, using view factor calculation configurations shown in Fig. 1 a) and b) in combination with the semi-circular approximation for the side extent;

Method 3 - detailed calculation based on the points positioned along the opening horizontal centreline in the middle, quarters and at the edges with the approximation of the side extent by an angular shape (Kučera, 2009) (Fig. 3 c) - the values of separation distances are established for the radiating surface horizontal centre line, using view factor calculation configurations shown in Fig. 1 a) and b) in combination with the angular approximation (equation (7)) for the side extent;

Method 4 - detailed calculation based on 100 evaluation points along the width (horizontal centreline) of the opening and additional 0.01 m increments to establish the side extent (Fig. 3 d) - the values of separation distances are established for the radiating surface horizontal centre line, using view factor calculation configurations shown in Fig. 1 a), b) and c).

Calculations described in items 2. and 3. are self-contained programmes, and method 4. was scripted in Python.

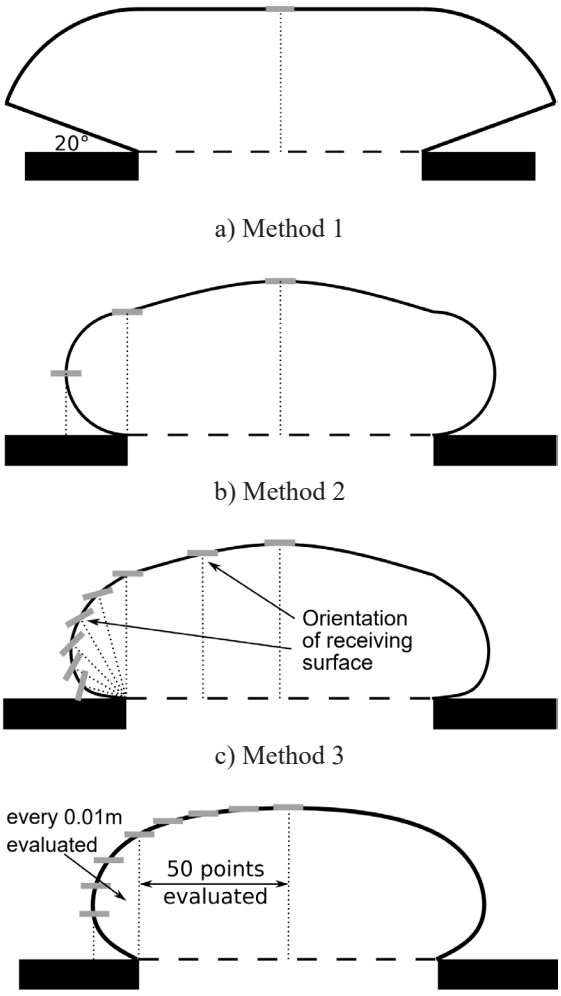

a) Method 1

b) Method 2

c) Method 3

d) Method 4

Fig. 3 Graphical representation of radiation intensity calculation methods

In addition to the analytical calculation methods and simplified tabulated approach radiation intensity was evaluated also in the Fire Dynamics Simulator (FDS) developed by the National Institute of Standards and Technology (NIST). It is a freely available simulation software which is complemented by a visualisation postprocessor Smokeview (NIST, 2020).

The individual calculation methods result in different shapes (extent) of the zone in which the radiation intensity is above the critical value of 18.5 kW.m^{-2}. This is apparent from Fig. 3 and is caused by the simplifications and number of evaluation points in the evaluation methods.

Method 1 (Fig. 3 a) is the most onerous one since the entire zone is based on one evaluation point. This point is located in the centre of the emitting surface and represents the highest exposure. The separation distance s is then projected from this point along the entire opening and to its sides up to an angle of 20°. It should be noted, that the separation distances were based using 100 %-open radiating surfaces, i.e. the worst-case scenarios for a particular length and width within the tabulated values. These were selected as the nearest greater values to the actual dimensions of the radiating surface (opening).

Method 2 (Fig. 3 b) evaluates the separation distance s in the centre of the opening as well as at its edges. Then a curve is projected through the three points obtained to obtain approximate values for the remainder of the opening width. The zone by the sides of the opening is projected as semi-circles with a diameter, which is equal to the separation distance calculated at the edge of the opening. Further description of this calculation method may be found in (Pokorný, 2017).

Method 3 (Fig. 3 c) the uses three evaluation points along the width of the opening - at the edges and in ¼, ½ and ¾ of the width. The zone by the sides of the opening is represented by a curve projected through evaluation points based at the edge of the opening and with varying exposure angle, i.e. the receiving surface is gradually tilted from 0° to 90°, in 10° increments. The resulting intensity beyond the edges of the opening Iθ is calculated using the Lambert's cosine law, using Equation (10). The program that calculates separation distances using this method rounds the results to 0.1 m, which leads to somewhat coarser results.

$$I_\theta = I \cdot \cos\theta \qquad [\text{kW.m}^{-2}] \ (10)$$

Method 4 is an implementation of equations (1)-(6) and (8)-(9) into the Python programming language. The objective was to maintain the parallel orientation of the receiving surface for all positions (within, at edges and outside the radiating surface). This was due to the fact that the receiving surface's shape/orientation does not usually change for one case. The number of evaluation points is explained above. This approach was adopted from Annex A of External Fire Spread - Building Separation and Boundary distances (Chitty, 2014).

For comparison with the four analytical methods an evaluation using CFD simulation in the Fire Dynamics Simulator was conducted. The computation mesh had a cell size of 25×25×100 mm. The configuration of the radiating surface was identical to the above described scenarios for analytical calculations. The entire radiating surface had a uniform temperature according to the ISO 834 time-temperature curve - 902.34 °C representing the 45th minute of a fully developed fire. Similarly to the analytical calculation methods, radiation intensity was monitored along on a plane aligned with the horizontal centreline. This was done in two different ways:

1. INTEGRATED INTENSITY - the command monitors the overall radiant heat flux received at any point in the plane from all directions. This spatial integration of received radiant heat flux at each point served as a reference of the maximum radiant heat exposure any point is able to receive.
2. RADIATIVE HEAT FLUX GAS - the command represents a radiometer of a given orientation. Therefore, the measuring point receives radiant heat flux with respect to its orientation. This is an analogy to the infinitely small fragment of receiving surface, which is used in the analytical methods.

Since FDS uses a different radiation heat transfer model, the shape of critical radiation intensity boundaries are slightly different. Its resolution and accuracy is dependent on the level angular discretisation, i.e. into how many spatial angles the computational domain is divided (NIST, 2020).

Results

The results obtained through the calculation methods and simulations described above are summarised in Table 1. The table has three parts which indicate the determined separation distances for the following:

- centre of the radiating surface (opening) with maximum heat radiation intensity;
- edges of the radiating surface (opening);
- side projection beyond the edges of the radiating surface (opening).

The results for the centre of the radiating surface (opening) indicate a relatively good agreement in the evaluated range. The maximum difference is between Method 1 (interpolation of tabulated data) and Integrated intensity from FDS for the width of 3 m - 0.21 m. Overall the differences are smaller than 10 %.

Safety Engineering Series, ISSN 1805-3238 pp. 38-46, DOI 10.35182/tses-2020-0005

Greater differences may be observed at the edges of the radiating surface. Due to the simplification of Method 1, the separation distances are identical to the values for the centre of the opening. The maximum difference between Method 1 and other analytical methods is 0.69 m and the minimum 0.17 m. The other analytical Methods (2-4) results show again a relatively good agreement with maximum differences of 0.1 m, which is less than 10 %. Greater differences may be also observed when the analytical Methods 2-4 results are compared to the simulation results, where they range from approx. 0.1 m to 0.3 m; significant differences are also present among the results from CFD simulations approx. 0.3 m to 0.5 m.

The most significant differences are present in the results for the projection of the heat radiation beyond the edges of the radiating surface (to the sides of the opening). The separation distances obtained from Method 1 are 2-times greater than those calculated using Methods 2-4. Interestingly, the Integrated intensity FDS results are smaller than those obtained from Methods 1-4.

To evaluate whether the analytical calculation results differences hold similar trends for larger radiating surfaces, the width of the opening was further increased up to 10 m. This was done in 1 m increments. The results are presented in Tab. 2. With the exception of Method 1 the differences among the other methods are relatively small and range from 0.01 m to 0.1 m at both evaluation points - radiating surface centre point and its edges.

Tab. 1 Separation distances obtained through calculations and simulations

Opening width	**Separation distance [m]**					
	Analytical calculations				**CFD simulation**	
	Method 1	**Method 2**	**Method 3**	**Method 4**	**Integrated**	**Radiometer**
In the centre of the radiating surface (maximum intensity)						
1.00	1.37	1.40	1.40	1.39	1.50	1.28
1.50	1.68	1.70	1.70	1.70	1.80	1.57
2.00	1.92	1.95	2.00	1,94	2.15	1.82
2.50	2.12	2.15	2.20	2.14	2.30	2.08
3.00	2.29	2.30	2.40	2.31	2.50	2.25
At the edges of the radiating surface						
1.00	1.37	1.20	1.30	1.21	1.35	1.08
1.50	1.68	1.40	1.40	1.40	1.55	1.26
2.00	1.92	1.50	1.60	1.51	1.75	1.32
2.50	2.12	1.55	1.60	1.58	1.85	1.37
3.00	2.29	1.60	1.70	1.63	1.90	1.43
To the sides of the radiating surface						
1.00	1.29	0.60	0.65	0.72/0.28*	0.50	0.20
1.50	1.58	0.70	0.71	0.76/0.31	0.55	0.25
2.00	1.80	0.75	0.78	0.81/0.32	0.60	0.26
2.50	1.99	0.78	0.78	0.77/0.33	0.70	0.27
3.00	2.15	0.80	0.85	0.84/0.33	0.60	0.28
*The separation distance (value in front of the slash) is shown at the maximum distance from the edge of the radiating surface where the radiation intensity reaches the limit of 18.5 $kW.m^{-2}$.						

Tab. 2 Separation distances obtained through analytical methods

Opening width	Separation distance [m]			
	Method 1	Method 2	Method 3	Method 4
In the centre of the radiating surface (maximum intensity)				
5.00	2.76	2.80	2.80	2.79
6.00	2.91	2.95	3.00	2.95
7.00	5.37	3.05	3.10	3.08
8.00	5.73	3.15	3.20	3.17
9.00	6.10	3.25	3.30	3.25
10.00	6.28	3.30	3.40	3.32
At the edges of the radiating surface				
5.00	2.76	1.70	1.70	1.70
6.00	2.91	1.70	1.70	1.71
7.00	5.37	1.70	1.80	1.72
8.00	5.73	1.70	1.80	1.72
9.00	6.10	1.70	1.80	1.72
10.00	6.28	1.70	1.80	1.72

Discussion

The results presented in the previous chapter provide a useful insight into the various calculation approaches to the determination of separation distances.

From a practical standpoint the analytical methods are the mostly used ones, however, the differences between the tabulated values (Method 1) and detailed calculations (Methods 2-4) are quite significant.

Method 1 is significantly more onerous at the edges and sides of the radiating surface. This is an expected result due to the simplification of this method. It takes the centre point (most intensive radiation) as representative of all points along and to the sides of the radiating surface. The differences at the edges range significantly from 10 % for the 1 m-wide opening to 90 % for the 10 m-wide opening. Beyond the opening width of 3 m, the tabulated values intervals become much coarser which is another source of significant overprediction. This overprediction is even more pronounced on the sides of the radiating surface where it ranges from 115 % to 170 %.

The differences among the detailed analytical Methods 2-4 are relatively small, in general between 0.01 m and 0.1 m, i.e. well under 10 %. Therefore, they may be considered equally accurate considering the overall accuracy at the scale of measurements of the building and its surroundings. The calculations along the width of the radiating surface are the same, so the differences are caused primarily by the rounding of input and output values.

Similarly, the differences resulting from the different approximations of the zones to the sides from the radiating surface do not appear to be significant among Methods 2-4. With the maximum difference of 0.12 m there is a good agreement among the methods within the evaluated range.

CFD simulations exhibit greater differences, both from the analytical methods as well as between the Integrated intensity and Radiometer heat flux measurements. Integrated intensity tends to overpredict the separation distance[1] in the centre and at the edges of the radiating surface slightly, by approx. 5-10 %, when compared to analytical Methods 2-4. On the other hand, Integrated intensity underpredicted the separation distances on the sides of the opening by about 20 %, when compared to analytical Methods 2-4.

The radiometer measurements (RADIATIVE HEAT FLUX GAS) were below the analytical methods and Integrated intensity in all cases. About 5-10 % for the centre, 10-15 % for the edges and 70 % for the sides of the radiating surface.

The main explanation for the differences is the different calculation approach when the CFD simulations are compared to the analytical methods. In addition the shape of the produced separation distance boundary, i.e. the extent beyond the risk

[1] At I_{crit} = 18.5 kW.m^{-2}.

of fire spread is considered sufficiently low, is not a smooth curve (e.g. Fig. 3 d), but rather a sinusoidal shaped one. This would require further smoothing to obtain better results.

This sinusoidal shape is explained in FDS Verification guide (McGrattan et al., 2020) and its extent depend on the number of the spatial angles. By increasing the number of spatial angles, the shape becomes smoother, however, the computational demand increases too. This dependence is shown in Fig. 4. Hence, when using FDS as a tool for separation distance prediction, the has to be aware of this effect and evaluate the predicted critical heat flux boundary in detail. In the investigated range, this approach resulted in underprediction when radiation intensity was monitored by radiometers - refer to Tab. 1, column Radiometer.

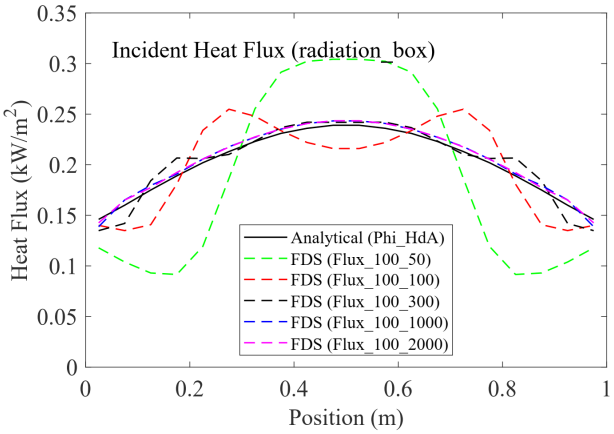

Fig. 4 Dependence of incident radiant heat flux prediction on the number of spatial angles in the range of 50-2000 in Fire Dynamics Simulator (McGrattan et al., 2020)

Conclusion

Fire separation distances are an important part of building fire safety design. They prevent fire spread in exterior primarily through radiating heat from fire but also falling burning brands. This paper analysed a number of methods for determination of required fire separation distances - tabulated values, analytical calculation methods and CFD simulations.

It was found that the tabulated values tend to overpredict the fire separation distances when compared to the other analytical and CFD methods; in some cases of larger radiating surfaces quite significantly. It could, be however, used as a quick preliminary assessment tool with a good margin of safety under the condition that 100 %-fire open radiating surfaces are considered.

CFD simulations proved computationally intensive and the results would require further processing. Alternatively, the number of spatial angles could be increased, however, this would increase the computational demand of the simulations even further. Hence, FDS did not prove a practical tool for the sole purposes of separation distances determination. It can be, of course, very helpful, in cases when CFD fire simulation is desired, however, the user should carefully determine the appropriate number of spatial angles for the radiation sub-model.

Finally, all three analytical calculation methods (Methods 2-4) proved to be more or less equally accurate and appropriate for the determination of fire separation distances. Since they are based on the same calculation principles as the tabulated values, their use is appropriate and in compliance with the national fire safety design standards. The increased resolution of these methods, particularly at the edges and sides of the radiating surface (opening), allows for more precise design.

References

Blahož, V., Kadlec, Z. 1996. Introduction to Heat Transfer. Ostrava: Association of Fire and Safety Engineering. ISBN 978-80-902001-1-1. (in Czech)

Chitty, R. 2014. External fire spread: building separation and boundary distances. 2. ed. Bracknell: IHS BRE Press. BR, 187. ISBN 978-1-84806-319-8.

ČSN 73 0802:2020. Building fire safety - Non-industrial buildings ed.2. (in Czech)

ČSN 73 0804:2020. Building fire safety - Industrial buildings ed.2. (in Czech)

ČSN EN 1991-1-2:2004. Eurocode 1: Actions on structures - Part 1-2: General actions - Actions on structures exposed to fire.

Kučera, P., Kaiser, R., Pokorný, J., Pavlík, T. 2009. Fire Engineering: Fire Dynamics. Ostrava: Association of Fire and Safety Engineering. ISBN 978-80- 7385-074-6. (in Czech)

NIST - National Institute Of Standards And Technology. FDS and Smokeview [software]. U.S. Department od Commerce, 2020 [cit. 2020-12-02]. Available at: https://pages.nist.gov/fds-smv/.

McGrattan, K., McDermott, R., Vanella, M., Hostikka, S., Floyd, J. 2020. Fire Dynamics Simulator Technical Reference Guide Volume 2: Verification [online]. U.S. Department of Commerce, National Institute of Standards and Technology, 2020 [cit. 2020-12-02]. Available at: https://pages.nist.gov/fds-smv/manuals.html.

Pokorný, M. 2017. Calculation of fire separation distances for radiatiant heat exposure [software]. (in Czech)

Reichel, V. 1989. Fire safety design of industrial buildings. IV. Praha: Czech national insurance institute. Loss prevention, 27. (in Czech)